Cervical mucosal inflammation expands functional polymorphonuclear myeloid-derived suppressor cells

Authors: Daan K.J. Pieren[1], Aleix Benítez-Martínez[1], Vicente Descalzo[1], Maider Arando[1], Patricia Álvarez-López[1], Jorge N. Garcia-Perez [1], Núria Massana[1], Júlia Castellón[1], Yannick Hoyos-Mallecot[2], Daniel Alvárez-Sierra[3]†, Clara Ramírez-Serra[4], Nuria Laia Rodriguez[5], Laura Mañalich-Barrachina[2], Cristina Centeno-Mediavilla[2], Josep Castellví [6], Vicenç Falcó[1], María J. Buzón[1], Meritxell Genescà[1]*

Affiliations:

[1]Department of Infectious Diseases, Hospital Universitari Vall d'Hebron, Institut de Recerca (VHIR), Universitat Autònoma de Barcelona; Barcelona, Spain.

[2]Microbiology Department, Hospital Universitari Vall d'Hebron; Barcelona, Spain.

[3]Diagnostic Immunology Group, Vall d'Hebron Institut de Recerca (VHIR), Vall d'Hebron Hospital Universitari, Vall d'Hebron Barcelona Hospital Campus; Barcelona, Spain.

[4]Clinical Biochemistry Research Group, Vall d d'Hebron Research Institute (VHIR), Biochemical Core Facilities, Vall d'Hebron University Hospital, Universitat Autònoma de Barcelona; Barcelona, Spain.

[5]Department of Obstetrics and Gynecology, Hospital Universitari Vall d'Hebron, Universitat Autònoma de Barcelona; Barcelona, Spain.

[6]Department of Pathology, Hospital Universitari Vall d'Hebron, Universitat Autònoma de Barcelona; Barcelona, Spain.

†Current address: Immunopathology Group, Instituto de Investigación Sanitaria Valdecilla (IDIVAL); Santander, Spain.

*Corresponding Author: Meritxell Genescà. Email: meritxell.genesca@vhir.org

One Sentence Summary: Suppressive myeloid-derived cells expand in the female genital tract mucosa under inflammatory conditions including presence of mucosal IL-1β.

Abstract: Microbial imbalance in the female genital tract increases the risk for adverse health outcomes in women and may increase susceptibility to genital tract infections. The local mucosal immune system plays a fundamental role in maintaining microbial balance. Among different relevant immune subsets, inflammation-induced myeloid-derived suppressor cells (MDSCs) remain understudied in the context of female genital tract conditions. Here we show that frequency of an MDSC subset, Polymorphonuclear (PMN-) MDSCs, increased in the cervical mucosa, but not in blood, of women with *Chlamydia trachomatis*, bacterial vaginosis, or with a coinfection, but not in women with human papillomavirus. Mucosal PMN-MDSC frequencies correlated with mucosal IL-1β in *C. trachomatis* patients and e*x vivo* exposure of cervical tissue to *C. trachomatis* elevated both PMN-MDSC frequencies and IL-1β secretion. Likewise, exposure of cervical tissue to cervicovaginal lavage fluid from *C. trachomatis* and bacterial vaginosis patients also enhanced PMN-MDSC frequencies. Lastly, cervical MDSCs expressed suppressive mediators and functionally suppressed cytotoxic T-cell responses. Our study identifies IL-1β-stimulated PMN-MDSCs as an immune suppressive mediator in female genital tract infections, potentially contributing to susceptibility to acquiring secondary infections at this site.

Main text:

INTRODUCTION

Microbial disturbances of the female genital tract (FGT) caused by bacterial vaginosis and sexually transmitted infections (STIs) have a detrimental impact on women's health, including genital tract inflammation, infertility, adverse birth outcomes, and cancer (*1, 2*). Furthermore, bacterial vaginosis and STIs such as *Chlamydia trachomatis*, or human papillomavirus may enhance susceptibility to acquiring secondary STIs (*3, 4*). A better understanding of immunological factors in the FGT initiated by microbial disturbances is vital to identify cells that may contribute to enhanced susceptibility to secondary STIs.

Inflammation of the FGT caused by bacterial vaginosis (BV) (*5-7*), *Chlamydia trachomatis* (CT) (*8*), human papillomavirus (HPV) (*9, 10*), and other pathogenic infections has been shown to enhance the risk of acquiring secondary STIs, such as HIV (*3, 4, 11-13*). Infection of the FGT with CT or other pathogens may lead to elevated levels of inflammatory cytokines and chemokines, such as GM-CSF, IL-1β, MIP-1α, MIP-1β, IP-10, IL-8, and CCL2 (*14-16*). Release of these signals may in turn attract $CD4^+$ T cells towards the cervical mucosa as target cells for HIV, as shown for CT infection (*17*), thereby predisposing for enhanced HIV susceptibility. However, these cytokines and chemokines may also attract and influence other local immune cell populations that may contribute to enhanced susceptibility to HIV.

Myeloid-derived suppressor cells (MDSCs) are myeloid cells developed as a consequence of pathology and may exert potent immune suppressive capacities. Presence of MDSCs has been described in a wide range of inflammatory diseases, spanning from cancer to infectious and autoimmune diseases (*18-20*) and develop under the presence of several cytokines and chemokines, including GM-CSF, VEGF, IL-6, IL-1β, and M-CSF (*18*). MDSCs have been classified to mainly consist of two subsets; a subset derived from monocytic myeloid lineages termed monocytic (M-) MDSCs, and a subset derived from granulocytic lineages termed polymorphonuclear (PMN-) MDSCs. These cells contain multiple mechanisms to exert immune suppression, which include expression of the enzyme indoleamine 2,3-dioxygenase (IDO) and the inhibitory ligand Programmed death-ligand 1 (PD-L1) (*21*). These

suppressive factors may limit cytotoxic functions of effector immune cells, including IFN-γ production and degranulation (*22-24*), required for effective elimination of infectious pathogens such as CT (*25-28*).

The role of MDSCs during FGT inflammation remains unexplored. Here, we investigated the presence of PMN- and M-MDSCs in the blood and cervical mucosa of women with multiple genital tract conditions. We found higher frequencies of PMN-MDSCs in the cervical mucosa of CT, BV, and coinfected patients associated to local changes that were not reflected in blood. Further, using an *ex vivo* cervical tissue model, we identified IL-1β as a main driver of PMN-MDSC activity in the context of CT infection. Our findings indicate a role for PMN-MDSCs during CT- and BV-induced cervical inflammation, potentially contributing to immune suppression at this mucosal site and thereby enhancing susceptibility to secondary STIs.

RESULTS

Study cohort

Paired PBMCs and plasma samples were acquired from peripheral blood in addition to cervical cytobrush and cervicovaginal lavage fluid from women suspected for having an STI. In total, 77 women were included in this study (**Fig. 1A**), from which part did not have a genital infection (Healthy donors, HD, n=18), or had a laboratory confirmed human papillomavirus infection (HPV, n=20), *Chlamydia trachomatis* infection (CT, n=14), *Gardnerella* bacterial vaginosis (BV, n=14), or a coinfection of CT, BV, and/or candidiasis (Coinf, n=11). Patient group characteristics including age, phase of the menstrual cycle and other parameters are presented in **Supplementary Table 1**. Of note, women assigned to the CT and Coinf groups were in general younger than women in the other groups. Menstrual cycle stages S1/S2 and S3/S4 showed a trend towards difference between groups (**Supplementary Table 1**).

PMN-MDSC frequencies are increased in the cervical mucosa of women with C. trachomatis, bacterial vaginosis, and coinfections

To investigate the role of MDSCs during FGT inflammatory conditions, we analyzed the presence of M-MDSCs and PMN-MDSCs in PBMC and cervical samples of recruited participants by flow cytometry. In these samples, we characterized M-MDSCs as $CD33^{+}CD11b^{dim/+}HLA\text{-}DR^{dim}CD14^{+}$ cells, and PMN-MDSCs as $CD33^{+}CD11b^{dim/+}HLA\text{-}DR^{-}CD14^{-}CD15^{+}$ cells (*21*) (**Fig. 1B**), after gating for single viable myeloid cells (**Supplementary Fig. 1A and 1B**). We first compared the frequency of M-MDSCs and PMN-MDSCs between blood and the cervical mucosa, as the frequency of immune cell subsets may differ across compartments. We observed comparable frequencies of M-MDSCs in PBMC and cervical samples across all groups, whereas PMN-MDSC frequencies were significantly higher in the cervical mucosa compared to PBMCs (**Fig. 1C**). We then assessed whether an FGT infection or an inflammatory condition alters the frequency of these MDSC subsets. In the cervical mucosa, we found that the frequency of PMN-MDSCs but not M-MDSCs was increased in BV, CT, and Coinf patients compared to HD (**Fig. 1D**). In contrast, M-MDSC but not PMN-MDSC frequencies tended to increase

in PBMCs of CT patients compared to other groups, although this trend was only significant when compared to the HPV group (**Fig. 1E**). In the cervical mucosa and PBMCs from HPV patients we did not observe any changes in MDSC subset frequencies compared to HD (**Fig. 1D, 1E**). Of note, age showed a negative association with cervical PMN- but not M-MDSC frequencies amongst all patients (**Supplemental Fig. 2A**). However, this was likely an effect of the younger age of the CT and Coinf patients included, who had higher PMN-MDSC levels. Indeed, to disentangle the effect of age on the observed differences, we performed a post hoc analysis to determine the frequency of cervical PMN-MDSC based on age (**Supplemental Fig. 2B**). When all samples were separated into patients who were above or below the median age (30 years old) no differences were observed (**Supplemental Fig. 2B**). In addition, we also confirmed that differences between groups that showed increased cervical PMN-MDSC frequencies, CT/BV/Coinf groups, and groups with low frequencies, HD/HPV groups, were maintained regardless of being younger or older than 30 years old (**Supplemental Fig. 2B**). Last, menstrual cycle stage did not appear to influence PMN- and M-MDSC levels (**Supplementary Fig. 2C**). However, by pooling and comparing HD/HPV groups versus CT/BV/Coinf groups, higher levels of PMN-MDSCs in the CT/BV/Coinf groups were maintained regardless of the menstrual cycle phase (**Supplementary Fig. 2C**).

Additionally, we addressed the presence of several other cell subsets in PBMCs and cervical mucosa of these patients (**Supplementary Fig. 3, 4**). The CT group exhibited more changes compared to HD than any other group: in the cervical compartment, the frequency of neutrophils and the expression of CD69 in $CD56^{dim}CD16^{+}$ NK cells were higher (**Supplementary Fig. 4A**); while in PBMCs, expression of CD69 was elevated in $CD56^{hi}CD16^{-}$ NK cells and lower frequencies of HLA-DR^{+} expression were detected in both NK cell subsets (**Supplementary Fig. 4B**). Similarly, BV and Coinf groups showed increased expression of CD69 in $CD56^{hi}CD16^{-}$ NK cells from PBMCs only, while lower frequencies of HLA-DR^{+} expression were detected in this same subset only in the BV group (**Supplementary Fig. 4B**). Last, the HPV group showed enhanced T cell expression of HLA-DR in the cervical samples compared to HD (**Supplementary Fig. 4A**), while no changes in other subsets from PMBCs were

observed for these women (**Supplementary Fig. 4B**). Together, we identify increased frequencies of PMN-MDSC associated to BV, CT, and coinfection that can only be detected at the local mucosa.

Cytokine profiles in CVL fluid of women with genital tract inflammation

To assess whether a specific cytokine microenvironment associated to MDSC levels, we measured cytokine levels in cervicovaginal lavage (CVL) fluid from our patients. These cytokines included growth factors (M-CSF, G-CSF, GM-CSF, and VEGF-A), inflammatory cytokines (IL-1β, IL-6, and TNF-α) and an anti-inflammatory cytokine (TGF-β1), which have been associated to MDSC development, expansion, and suppressive activity (*18*). BV patients showed higher levels of M-CSF, GM-CSF, VEGF-A, IL-1β, and TGF-β1 compared to HD (**Fig. 2A**). In contrast, CT patients only showed higher levels of M-CSF compared to HD. Coinf patients showed increased levels of M-CSF, but also GM-CSF, and IL-1β, while HPV patients did not show any differences compared to HD (**Fig. 2A**). In contrast, cytokine levels in plasma samples did not show major differences between HD and the other groups, aside from an increased level of TGF-β1 in the Coinf group (**Supplementary Fig. 5**).

Next, we assessed whether levels of specific cytokines in the CVL fluid associated with higher frequencies of PMN-MDSCs detected in the cervical mucosa of BV, CT, and Coinf patients as observed in **Fig. 1D**. Amongst all patients included in our study, only the level of M-CSF present in CVL fluid positively correlated with the frequency of PMN-MDSCs in the cervical mucosa (r 0.45, $p<0.001$) (**Supplementary Table 2**). However, when analyzing within each group of patients, only HPV reflected this finding (r 0.74, $p=0.04$). Aside from negative correlations within the HD group, likely caused by low levels of cytokines and low PMN-MDSC frequencies (**Supplementary Table 2**), we observed strong positive correlations between the level of IL-1β found in the CVL of CT patients and the frequency of PMN-MDSCs, while for BV patients the level of VEGF-A positively correlated with the frequency of PMN-MDSCs (**Fig. 2B**). Together these data suggest that IL-1β in CT patients and VEGF-A in BV patients could, in part, contribute to the accumulation of PMN-MDSCs found in the cervical mucosa.

Ex vivo exposure of cervical tissue to C. trachomatis elementary bodies expands the PMN-MDSC subset and increases levels of IL-1β

As we observed expansion of PMN-MDSCs in the cervical mucosa of CT patients, we next explored whether *ex vivo* exposure of cervical tissue to infectious elementary bodies (EBs) of *C. trachomatis* could reproduce this PMN-MDSC expansion. Exposure of cervical tissue to EBs induced higher frequencies of PMN-MDSCs compared to the control (**Fig. 3A, 3B**). Exposure to GM-CSF and IL-6, previously reported as MDSC developmental factors (*18*), also induced a trend towards higher levels of PMN-MDSCs (**Fig. 3A, 3C**). In contrast, the frequency of M-MDSCs showed a trend towards lower levels in cervical tissue as a consequence of exposure to either EBs or GM-CSF with IL-6 (**Fig. 3A, 3B, 3C**).

PD-L1 and IDO are two phenotypical markers that indicate suppressive MDSC potential (*21*). Therefore, we determined whether cervical exposure to CT EBs also altered the suppressive phenotype of tissue-derived MDSCs. We observed a trend towards increased frequencies of PD-L1$^+$ PMN-MDSCs and M-MDSCs after exposure to EBs (**Fig. 3D, 3E**). In addition, M-MDSCs but not PMN-MDSCs showed a trend towards higher levels of IDO$^+$ and IDO$^+$PD-L1$^+$ double positive cells (**Fig. 3D, 3E**).

Last, we measured the level of cytokine concentrations in the culture supernatant to address whether secreted signals were similar to the cervical milieu detected in CT patients, thus potentially explaining expansion of PMN-MDSCs in EB-exposed cervical tissue. Similar to the potential importance of IL-1β found in the CVL fluid of CT patients (**Fig. 2B**), the level of IL-1β was significantly higher upon exposure to EBs compared to the control (**Fig. 3F**). Additionally, levels of GM-CSF and TNF-α showed a trend towards higher levels upon exposure to EBs compared to the control (**Fig. 3F**), whereas levels of M-CSF, G-CSF, VEGF-A, IL-6, and TGF-β1 were not modified (**Supplementary Fig. 6**). Together, our data indicate that expansion of PMN-MDSCs as a consequence of CT exposure may be driven by IL-1β, which enhances expression of phenotypical markers of immune suppression on both PMN- and M-MDSCs.

CVL fluid of CT and BV patients and IL-1β recapitulate PMN-MDSC expansion in cervical tissue

To further investigate the potential link between the FGT inflammatory cytokine micro-environment and MDSC expansion and/or activity, we addressed whether CVL fluid from CT or BV patients or IL-1β were capable of inducing increased frequencies of PMN-MDSCs in cervical tissue. To this end, cervical tissue blocks were exposed to medium supplemented with CVL fluid from CT or BV patients, IL-1β, or HD CVL as a control for 24 hours. CVL fluid of CT and BV patients induced higher levels of PMN-MDSCs in cervical tissue compared to tissue exposed to HD CVL fluid (**Fig. 4A, 4B**). In contrast, tissue M-MDSC frequencies did not change in response to CT CVL fluid, while M-MDSC levels decreased when exposed to BV CVL fluid (**Fig. 4C**). Additionally, direct exposure of cervical tissue to IL-1β resulted in a similar effect, showing a trend towards increasing PMN-MDSC (**Fig. 4B**) but not M-MDSC frequencies compared to the HD control (**Fig. 4C**).

Similar to EBs of *C. trachomatis* (**Fig. 3F**), tissue exposure to CT CVL fluid showed a trend towards higher levels of PD-L1^{+} PMN-MDSCs but not IDO^{+} PMN-MDSCs (**Fig. 4D**). Moreover, CT CVL fluid induced a trend towards higher levels of PD-L1^{+}IDO^{+} double positive PMN-MDSCs, while exposure to BV CVL fluid did not (**Fig. 4D**). In contrast, M-MDSCs showed higher frequencies of PD-L1^{+}, IDO^{+}, and PD-L1^{+}IDO^{+} double positive cells in response to CT and BV-derived CVL fluid, as well as IL-1β (**Fig. 4E**). Of note, the effect of IL-1β increasing the potential suppressive capacity of PMN-MDSCs, but not the increase of their frequency, was confirmed in PBMCs exposed to IL-1β (**Supplementary Fig. 7**). Together, these findings indicate that CVL fluid of CT and BV patients may contain a specific cytokine micro-environment that results in increased frequencies of PMN-MDSCs, which may be partially driven by presence of IL-1β.

Cervical MDSCs suppress T-cell activation and cytotoxic potential

MDSCs isolated from peripheral blood have previously been shown to suppress T-cell cytotoxic responses and proliferation (*22, 23, 29*). However, the suppressive activity of MDSCs residing in cervical tissue has not been addressed. We therefore investigated the suppressive capacity of MDSCs derived from non-tumoral cervical tissue of patients undergoing surgery, from which T cells and MDSCs were isolated from single cell suspensions by cell sorting. To determine repression of T cell cytotoxic factors, we assessed expression of IFN-γ, Granzyme B and degranulation marker CD107a, after stimulation with anti-CD3/anti-CD28 beads overnight with or without the presence of MDSCs (**Fig. 5A**). Addition of MDSCs to the T-cell cultures resulted in significant or a trend towards significant suppression of $CD8^+$ and $CD4^+$ T cells degranulating ($CD107a^{hi}$) in combination with expression of CD69 or Granzyme B (**Fig. 5B**). Additionally, MDSCs suppressed the frequency of $CD107a^+$ $CD8^+$ T cells while in some samples IFN-γ^+ $CD4^+$ T cells (in three out of five) and granzyme B^+ $CD4^+$ T cell frequencies (in three out of six) were also suppressed. Of note, cell yield limited discerning between MDSC subsets for these analyses.

Last, to translate these findings to the patients included in our study, we assessed associations between the presence of PMN- and M-MDSCs in the cervical mucosa with the frequency of $CD69^+$ T cells, indicative of T cell activation and/or tissue residence (*30, 31*). Amongst all women included in our study we did not find an association between the frequency of cervical mucosa PMN-MDSCs and $CD69^+$ $CD4^+$ T cells (**Fig. 5C**). However, in CT patients, we observed a negative correlation between the frequency of cervical mucosa PMN-MDSCs and $CD69^+$ $CD4^+$ T cells (**Fig. 5C**). Together, these data indicate that MDSCs residing in cervical mucosa suppress antimicrobial effector functions of cervical $CD4^+$ and $CD8^+$ T cells.

DISCUSSION

Inflammation of the cervical mucosa increases the risk for adverse health outcomes in women. Changes to the local immune micro-environment may hamper resolution of ongoing infections, increase the vulnerability to secondary FGT infections, such as HIV (*3, 4, 6-9, 11, 13*), and may contribute to infertility and preterm labor (*32*). Insight into the immunological cell subsets present at the cervical mucosa during inflammatory conditions is important for patient treatment as well as for development of new therapies and ongoing vaccination development against STIs, such as CT (*33*). Here, we identified that CT, BV, and coinfections expand the level of functional PMN-MDSCs in the cervical mucosa, thereby likely reducing time to pathogen clearance while potentially enhancing vulnerability to secondary infections at this site and compromising overall reproductive health.

Whereas most studies assessed MDSC presence in blood, we observed higher levels of PMN-MDSCs in the cervical mucosa compared to blood across all patient groups, which were accompanied by inflammation-induced changes at the cervical mucosal site but not systemically. These findings indicate that in compartmentalized mucosal- and tissue-specific conditions, assessment of the presence and role of relevant immune subsets, such as MDSCs, requires studying the local environment rather than blood. However, M-MDSCs and PMN-MDSCs have previously been shown to increase in blood of COVID-19 patients but not in the airway mucosa, while for influenza infected patients mucosal levels where higher compared to blood (*29*), indicating that not all infections elicit similar mucosal versus systemic alterations impacting MDSC levels. Of note, the level of localized versus systemic inflammation and sample timing may have an impact on these findings. Increased levels of PMN-MDSCs have previously been described in cancer, autoimmune disease (*18, 19*), COVID-19 (*29, 34*), and chronic viral infections such as HIV (*22, 35*). However, to date, the role of MDSCs in the context of localized genital tract inflammatory conditions in women remained unknown. In mice, a recent report showed that *in vivo* infection with CT increased levels of MDSCs in the cervix, which could be reversed by inhibition of the yes-associated protein 1 (*36*). However, due to a limited set of phenotypical markers used, subsets of MDSCs were not identified (*36*). We now show elevated PMN-MDSC levels in the cervical mucosa of women with CT, BV, and a coinfection, but not in women with HPV.

CT infection often presents as a silent, asymptomatic infection in women (*37*) as opposed to highly inflammatory genital conditions such as BV. This may explain why CVL fluid cytokine levels from CT patients in our study were not differing much from HD, in contrast to the CVL fluid of BV and Coinf patients. While M-CSF was the only molecule significantly increased in the CVL of CT women compared to HD, we detected a positive correlation between cervical mucosal IL-1β levels and PMN-MDSC frequencies in these CT patients. Indeed, IL-1β has been reported as a driver of suppressive PMN-MDSC expansion in tumor-bearing mice (*38, 39*), through activation of extracellular signal-regulated kinases 1 and 2 (*40*). Moreover, and similar to our findings, levels of IL-1β positively correlated with PMN-MDSC frequencies in the blood of COVID-19 patients (*41*). Altogether, our findings support the role of IL-1β as one of the drivers of CT-mediated PMN-MDSC expansion. In addition, IL-1β has been described as a potential inducer of PD-L1 and IDO expression in myeloid cells (*42, 43*). These findings warrant further exploration of blocking IL-1β and/or signaling pathways to reduce PMN-MDSC levels and activity. Nonetheless, other factors present in the cervical mucosal micro-environment may additionally contribute to expand PMN-MDSCs and/or modify their function (*18*).

In contrast to CT, patients with BV and Coinf showed elevated levels of several cytokines in the CVL fluid. Aside from our analyses on the effect of IL-1β, for BV, levels of VEGF-A were higher in their CVL fluid and correlated with increased levels of mucosal PMN-MDSCs. However, VEGF-A did not modify the frequency or potential suppressive capacity of PMN-MDSC in PBMCs. VEGF may function as a chemoattractant for MDSCs (*44*), and the attraction is further propagated by MDSC production of matrix metalloproteinase 9, which allows the release of VEGF into the micro-environment (*45*). Moreover, we found that exposure of cervical tissue to BV CVL fluid elevated PMN-MDSC frequencies, suggesting a role for the milieu signature associated to these samples in PMN-MDSC development, including VEGF-A. Whereas the composition of genital bacterial communities in the cervix determines the cytokine micro-environment (*6*), bacterial species other than *Gardnerella,* one of the main causative pathogens of BV, may also determine the level of PMN-MDSCs in the cervical mucosa. In contrast, CVL fluid cytokine levels and mucosal MDSC frequencies of the HPV patients

included did not seem to differ significantly from HD patients. Possibly, cellular and cytokine micro-environments are altered in these patients beyond the makers we addressed in this study (*14*). While MDSCs have been highlighted as a mechanism limiting cervical tumor clearance (*46*), women included in the HPV group of our study were diagnosed with low- or high-grade squamous intraepithelial lesions, but not with cervical cancer, potentially explaining unaltered levels of MDSCs compared to the control group. Indeed, HPV patients have been shown to accumulate MDSCs in the tumor (*47*).

Importantly, by isolating MDSCs from non-tumoral cervical tissue we were able to demonstrate the suppressive capacity of these tissue-resident MDSCs. We showed that MDSCs suppressed degranulation and cytotoxic factors of $CD4^+$ and $CD8^+$ T cells required for optimal pathogen clearance (*25, 26*), suggesting that MDSCs found in patients associated to some degree of FGT inflammation are suppressive. Due to limited availability of cervical tissue and sorted cell numbers, we were not able to separately analyze and compare the suppressive capacity of tissue-resident PMN- and M-MDSCs. Furthermore, we observed that *ex vivo* exposure of cervical tissue to CT EBs and CT CVL fluid induced higher frequencies of PD-$L1^+$ PMN-MDSCs and PD-$L1^+IDO^+$ M-MDSCs. Indeed, induction of IDO and PD-L1 enhances the immune suppressive capacity of MDSCs (*48, 49*). Our results indicate that, while only PMN-MDSCs are expanded after EB stimulation, both PMN-and M-MDSCs may increase their suppressive capacity as a consequence of exposure to CT. Moreover, exposure of cervical tissue to BV CVL fluid mainly increased frequencies of PD-$L1^+$ and IDO^+ M-MDSCs, suggesting an enhanced suppressive role of these cells in the context of BV. Further research should separately assess suppression by PMN-MDSC and M-MDSCs, as well as the capacity of these cells to suppress antigen-specific T-cell responses to CT and other inflammatory mediators. This would provide more insight into the suppressive role of these subsets during FGT inflammation. Nonetheless, our results indicate an effect of FGT inflammation on the suppressive capacity of both PMN- and M-MDSC subsets and warrant further exploration of reducing MDSC levels in the FGT during inflammation and blocking of suppressive mechanisms, such as PD-L1.

Whether age has an impact on PMN-MDSC frequencies in the cervical mucosa remains to be elucidated. While we observed a negative association between the level of cervical mucosa PMN-MDSCs and age,

higher levels of PMN-MDSCs in CT/BV/Coinf patients compared to HD and HPV samples were maintained regardless of age. Further, expansion of MDSCs has been reported to occur during aging in the blood and secondary lymphoid organs of mice (*50*), which is mainly explained by a chronic low-grade increase in levels of inflammatory cytokines during aging, including cytokines reported to promote MDSC expansion (*51*). Moreover, higher MDSC levels in the blood of COVID-19 patients have recently been shown to be associated with age (*29*). Thus, as age differed between our patient groups with younger ages present in the CT and Coinf groups, our findings indicate that higher levels of PMN-MDSCs in the groups with younger age were most likely caused by inflammation of the cervical mucosa rather than an age-related increase of PMN-MDSCs. Furthermore, MDSCs may expand due to changes to the cervicovaginal environment caused by estrogens (*52*) and pregnancy (*53*). Whereas we found a trend towards differences in menstrual cycle stages between groups, this did not appear to significantly change mucosal MDSC frequencies and, once again, differences were maintained when the two dominant phases of the menstrual cycle, follicular and luteal, were separated (*54*).

Overall, we demonstrate that CT, BV, and coinfections in the FGT expand PMN-MDSCs in the cervical mucosa and promote MDSC suppressive capacity. Further, both the expansion of PMN-MDSCs and enhanced activity may be in part driven by IL-1β in the cervical micro-environment. Differentiation and recruitment of MDSCs during inflammation in the FGT has likely evolved to prevent over-activation of effector cells and thereby tissue pathology. However, enhanced immune suppression may also negatively impact effector responses to pathogens, resulting in less efficient immune clearance while likely increase vulnerability to secondary STIs such as HIV. Our findings provide a starting point for designing preventive and therapeutic strategies limiting MDSC expansion induced by inflammatory mediators, which could improve natural pathogen clearance, potentially lowering antibiotic usage and resistance, and limiting vulnerability to secondary STIs. Altogether, we identified unique features of resident immune cells influenced by the local mucosal microenvironment crucial for enhancing mucosal immunity and ensuring sexual and reproductive health.

MATERIALS AND METHODS

Study Design

This study was designed to elucidate the role of MDSCs during female genital tract (FGT) inflammation. Women visiting the Drassanes Vall d'Hebron Centre for International Health and Infectious Diseases in Barcelona, Spain due to self-suspected FGT inflammation were included in this study and allocated to their study group after laboratory confirmed FGT condition. Inclusion criteria for the *C. trachomatis* group was confirmation by nucleic acid amplification test (NAAT). For the bacterial vaginosis group, inclusion criteria was presence of three out of four Amsel criteria, including thin, white, yellow, homogeneous discharge, clue cells on wet mount microscopy, a vaginal fluid pH of over 4.5 when placing the discharge on litmus paper or release fishy odor after adding 10% potassium hydroxide (KOH) solution to wet mount - also known as "whiff test", together with Ison-Hay criteria for suspected cases (*55*). The presence of *Candida spp*. was determined by culture. In addition, women with HPV infection diagnosed by the Hybrid Capture 2 system (Qiagen), followed by the CLART-HPV2 test (Genomica, Madrid, Spain), a polymerase chain reaction technique that allows the detection of 35 HPV genotypes, or by the Cobas HPV Test (Roche Molecular System), and women without STI or signs of FGT inflammation were recruited at the Gynecology and Obstetrics department of the Vall d'Hebron University Hospital (HUVH), Barcelona, Spain. Exclusion criteria were: HIV or hepatitis, immune-related illnesses, systemic illnesses, pregnancy, and menstruation at the time of visit. All women were asked to fill in a questionnaire, registering prior FGT inflammatory conditions and other immunological or allergic conditions, medication, menstrual cycle stage at time of the study and use of hormonal contraceptives. Healthy non-tumoral cervical tissue used in this study was obtained from patients recruited at the Gynecology Unit of the HUVH, undergoing a partial or radical hysterectomy for various reasons. Randomization and blinding were not performed for this study. Stopping the collection of data was based on a predefined sample collection period. Experiments were performed once per participant due to the limited availability of clinical samples. Low numbers of cellular subsets (<100 cells) in clinical samples detected by flow cytometry were excluded. For cytokine analyses specifically, extreme outliers were excluded based on the ROUT method (Q=0.1% to remove definitive outliers) in Prism

8.3.0 (GraphPad Software, La Jolla, CA, USA). Signed informed consent was obtained from all participants included in this study. This study was performed in accordance with the Declaration of Helsinki. Ethical approval was given by the corresponding Institutional Review Board (PR(AG)117/2018) of the Vall d'Hebron University Hospital (HUVH), Barcelona, Spain.

Sample collection

Whole blood from women with and without FGT conditions was collected in EDTA-containing tubes. Plasma was isolated from these samples and stored at −80°C. Subsequently, PBMCs were isolated via Ficoll–Paque separation. Part of these PBMCs were immediately used for flow cytometry analyses, while the rest was stored in liquid nitrogen. From the same women, an endocervical sample was collected with a cytobrush and cervicovaginal lavage (CVL) fluid was obtained by introducing 5mL of physiological serum into the cervicovaginal canal and the posterior fornix, after which the serum was retrieved again. Cervical samples were kept at 4°C and were sent to the laboratory for immediate processing (<4 hours after collection). Cervical cytobrush samples were vortexed, washed with PBS, filtered through a 100µm pore-size cell strainer (Labclinics), and centrifuged, before immediate labelling for flow cytometry. CVL fluid samples were centrifuged to remove mucus and debris. Subsequently, the supernatant was stored at −80°C, while remaining cells in the cell pellet were added to the cervical cytobrush samples.

Healthy endo- and ectocervical tissue was collected from patients at the HUVH undergoing partial or radical hysterectomy and stored in antibiotic-containing RPMI 1640 medium, after pathological inspection. Endo- and ectocervical tissue was immediately dissected into 8-mm^3 tissue blocks as reported previously (*31, 56*). Depending on the assay, tissue blocks were either immediately enzymatically digested or first cultured in several conditions described below before tissue digestion. Enzymatic digestion was initiated by adding 10 mg/mL collagenase IV (Gibco) in RPMI +5% FBS to the tissue blocks, incubated for 30 mins at 37ºC and 400 rpm before mechanically digestion with a pestle

(*31, 56*). Cell suspensions were filtered through a 70µm pore-size cell strainer (Labclinics) and prepared for flow cytometry as described below.

Flow cytometry of patient PBMC and Cytobrush

Single cell suspensions of PBMC and cytobrush samples were stained with Live/Dead Aqua (Invitrogen) before extracellular labeling with antibodies targeting the following proteins: CD33 (PerCP-Cy5.5, Clone WM53, Biolegend, #303414), CD11b (FITC, Clone M1/70, Biolegend, #101205), CD3 (PE-Cy7, Clone SK7, BD Biosciences, #557851), CD69 (PE-CF594, Clone FN50, BD Biosciences, #562617), CD56 (PE, Clone B159, BD Biosciences, #555516), CD14 (APC-H7, Clone MφP9, BD Biosciences, #560180), CD45 (AF700, Clone HI30, Biolegend, #304024), CD8 (APC, Clone RPA-T8, BD Biosciences, #561952), CD16 (BV786, Clone 3G8, BD Biosciences, #563690), CD103 (BV650, Clone Ber-ACT8, BD Biosciences, #743653), CD15 (BV605, Clone W6D3, BD Biosciences, #562980), and HLA-DR (BV421, Clone G46-6, BD Biosciences, #562804). Labeling was performed at room temperature for 20 mins, washed with PBS +3% FBS (PBMCs) or washed with PBS +3% normal mouse serum (NMS) and normal goat serum (NGS), and fixed with PBS+1% paraformaldehyde before acquisition on a BD LSR Fortessa flow cytometer (Cytomics Platform, High Technology Unit (UAT), Vall d'Hebron Institut de Recerca (VHIR)).

Measurement of cytokines

Cytokines present in the plasma and CVL fluid of FGT inflammatory patients as well as in *ex vivo* cervical tissue supernatants were detected using an automated multiplex ELISA system (Ella Simple Plex™, Bio-Techne R&D Systems). Levels of the following eight analytes were detected in these samples according to the manufacturer's instructions: M-CSF, G-CSF, GM-CSF, VEGF-A, IL-1β, IL-6, TNF-α, TGF-β1. Levels of analytes found in CVL fluid samples were corrected for the total amount of protein found in CVL fluid. Total protein content was measured using the Atellica CH automated equipment (Siemens Healthineers®) with a colorimetric methodology based on the biuret test.

Flow cytometry of cervical tissue

After digestion of cervical tissue blocks and depending on the assay, single cell suspensions were stained with Live/Dead Aqua (Invitrogen) before extracellular labeling with antibodies targeting the following proteins: HLA-DR (PerCP-Cy5.5, Clone G46-6, BD Biosciences, #560652), CD11b (FITC, Clone M1/70, Biolegend, #101205), PD-L1 (PE-Cy7, Clone 29E.2A3, Biolegend, #329718), CD14 (APC-H7, Clone MφP9, BD Biosciences, #560180), CD45 (AF700, Clone HI30, Biolegend, #304024), CD15 (BV605, Clone W6D3, BD Biosciences, #562980), and CD33 (BV421, Clone P67.6, Biolegend, #366622). Extracellular labeling was performed at room temperature for 20 minutes in PBS+ 3% NMS/NGS and washed with PBS +3% NMS/NGS. For intracellular antibody labeling, cells were fixed for 20 mins at RT (Medium A, Invitrogen) and labeled for the following proteins: IDO (PE, Clone eyedio, Invitrogen, #12-9477-42), ARG-1 (APC, Clone A1exF5, Invitrogen, #17-3697-80) in permeabilizing medium (Medium B, Invitrogen) for 30 minutes at RT. Cells were then washed with PBS +3% NMS/NGS, and fixed with PBS+1% paraformaldehyde before acquisition on a BD LSR Fortessa flow cytometer (Cytomics Platform, UAT, VHIR).

Purification of Chlamydia trachomatis elementary bodies and infection of cervical tissue

HeLa-229 cells (ATCC CCL-2.1) were infected with *C. trachomatis* Serovar D (ATCC VR-885) as previously described (*57*), with minor modifications. Briefly, HeLa 229 cells were maintained in DMEM (+10% FBS + penicillin/streptomycin) at 37ºC before chlamydia infection. To infect HeLa cells, confluent cell monolayers grown in 25cm^2 flasks (6x10^6 cells/well) and exposed to thawed *C. trachomatis* elementary bodies (EBs) in DMEM (+10% FBS +10µg/mL gentamycin +1µg/mL cycloheximide). Flasks were centrifuged (30 mins at 754 x *g*) and placed at 37ºC. After 48h of incubation and/or observation of the characteristic cytopathic effect (cytoplasmic inclusion bodies) in 90-100% of the infected cells, cells were collected into tubes by scraping and centrifuged at 400 x *g* for 7 mins to remove the supernatant. The cell pellet was resuspended in ice cold PBS, transferred to a bijou tube with 5-7 glass beads (Thermo Fisher, #11369123) and briefly vortexed. After centrifugation, the supernatant

was mixed 1:1 with sucrose-phosphate-glutamate buffer (SPG) and stored at -80ºC until further use. To titrate the infective stock, 1:10 serial dilutions were made in HeLa229 cells plated in a 96-well plate. After 48-72 h of incubation at 37°C and 5% CO2, infected cell monolayers were washed twice with PBS and fixed in 96% ice cold methanol for 10 min at -20°C. After washing and blocking unspecific unions with 3% BSA-PBS at RT for 60min, chlamydial inclusions were stained with FITC-conjugated anti-Chlamydia antibody (Chemicon #AB1120F; 1/200 dilution t RT for) at RT for 1h. Inclusions were counted by observation with a fluorescence microscope and results were expressed in inclusion forming units (IFU/ml).

For tissue infection, fresh ecto- and endocervical tissue blocks (8 mm^3) were placed in a 24 wells plate with the mucosa facing upwards and exposed to RPMI 1640 (+20% FBS, without penicillin) alone, or RPMI 1640 (+20% FBS) with *C. trachomatis* EB ($1*10^5$ IFU/mL) or GM-CSF (10 ng/mL) and IL-6 (10 ng/mL) directly placed into the mucosal interface and incubated for 48 hours at 37ºC After incubation, tissue blocks were digested and prepared for flow cytometry to assess MDSC frequencies and phenotype as described above.

Exposure of PBMCs to cytokines and growth factors

PBMCs derived from healthy women included in this study were seeded in triplicate in a 96-well plate ($2*10^5$ cells/well) in RPMI (+10% FBS + penicillin/streptomycin) alone, or supplemented with GM-CSF (10 ng/mL) + IL-6 (10 ng/mL), M-CSF (50ng/mL), VEGF-A (50ng/mL), or IL-1β (50ng/mL) for 48 hours at 37ºC. After incubation, triplicates were pooled and cell suspensions were prepared for flow cytometry to assess MDSC frequencies and extra- and intracellular phenotypes as described above.

Exposure of cervical tissue to CVL fluid

Cervical tissue blocks (8 mm^3) were placed in a 24-well plate in the presence of equal amounts of RPMI 1640 + 20% FBS and CVL fluid of CT, BV, or HD patients. Before use, CVL fluid samples were thawed

and centrifuged to get rid of potential debris. Additionally, cervical tissue was exposed to IL-1β (100 ng/mL). Cervical tissue blocks were then incubated for 24 hours at 37ºC. After incubation, tissue blocks were digested and prepared for flow cytometry to assess MDSC frequencies and phenotype, including intracellular markers, as described above.

MDSC suppression assay

Single cell suspensions of freshly obtained cervical tissue were stained with Live/Dead Aqua (Invitrogen) and extracellularly labeled with antibodies targeting the following proteins: HLA-DR (PerCP-Cy5.5, Clone G46-6, BD Biosciences, #560652), CD11b (FITC, Clone M1/70, Biolegend, #101205), CD14 (APC-H7, Clone MφP9, BD Biosciences, #560180), CD45 (BV605, clone HI30, BD Biosciences, #564047), CD20 (V500, Clone, BD Biosciences, #647463), and CD33 (BV421, Clone P67.6, Biolegend, #366622). Cell suspensions were then resuspended in PBS+3% FBS and sorted into lymphocyte (based on FSC and SSC size) and MDSC ($CD14^{+}$ and $CD14^{-}$ $HLA\text{-}DR^{Low}$ cells of $CD33^{+}CD11b^{+}$ myeloid cells) fractions using the Cytek Aurora Cell Sorter (Cytek Biosciences). Suppression assays were performed by culturing duplicates or triplicates of sorted lymphocytes with and without MDSCs in a ratio of 1:5 (MDSC:lymphocyte) in U-bottom 96-wells plates in the presence or absence of anti-CD3/anti-CD28 coupled beads (1:2 bead-to-lymphocyte ratio) (Dynabeads™, Invitrogen), CD107a (PE-Cy5, clone H4A3, BD Biosciences, #555802), brefeldin A (0.55 µL/mL), monensin (0.385 µL/mL) for 18 hours at 37ºC. After culturing, duplicates or triplicates were pooled, washed with PBS, and fixed and permeabilized for intracellular labeling (Foxp3/Transcription Factor Staining Buffer, eBioscience) with the following antibodies: CD69 (PE-CF594, clone FN50, BD Biosciences, #562617), Granzyme B (PE, Clone GB11, Thermo Fisher, #GRB04), IFN-γ (AF700, Clone B27, Invitrogen, #MHCIFG29), CD8 (APC, Clone RPA-T8, BD Biosciences, #561952), and CD3 (BV650, Clone UCHT1, BD Biosciences, #563851). Cells were acquired on a BD LSR Fortessa flow cytometer (Cytomics Platform, UAT, VHIR).

Statistical analyses

Data shown in bar graphs were expressed as median and interquartile range. Wilcoxon matched-pairs signed rank test was applied for paired comparisons. Kruskal–Wallis rank–sum test with Dunn's post hoc test was used for multiple comparisons. Correlation analyses were performed using non-parametric Spearman rank correlation. Linear regression analysis was performed to generate lines of best fit. Suppression in suppression assays were calculated as follows: ((% marker T cell only – % marker T cell with MDSC suppressor cells) / (% marker T cell only)) × 100%. Statistical significance was then determined by Wilcoxon matched-pairs singed rank test. A p value < 0.05 was considered statistically significant. No statistical method was used to predetermine sample size, as this was dependent on patient consent and eligibility to the study groups. Flow-cytometry data were analyzed using FlowJo v10.7.1 software (TreeStar). Data and statistical analyses were performed using Prism 8.3.0 (GraphPad Software, La Jolla, CA, USA).

List of Supplementary Materials

Fig. S1 to S7

Table S1 and S2

References

1. WHO, Sexually transmitted infections (STIs) (Fact sheet) (2023).
2. WHO, Bacterial vaginosis (Fact sheet) (2023).
3. M. Laga, A. Manoka, M. Kivuvu, B. Malele, M. Tuliza, N. Nzila, J. Goeman, F. Behets, V. Batter, M. Alary, W. L. Heyward, R. W. Ryder, P. Piot, Non-ulcerative sexually transmitted diseases as risk factors for HIV-1 transmission in women: results from a cohort study. *AIDS* **7**, 95-102 (1993).
4. K. Mlisana, N. Naicker, L. Werner, L. Roberts, F. van Loggerenberg, C. Baxter, J. A. Passmore, A. C. Grobler, A. W. Sturm, C. Williamson, K. Ronacher, G. Walzl, S. S. Abdool Karim, Symptomatic vaginal discharge is a poor predictor of sexually transmitted infections and genital tract inflammation in high-risk women in South Africa. *J Infect Dis* **206**, 6-14 (2012).
5. J. Atashili, C. Poole, P. M. Ndumbe, A. A. Adimora, J. S. Smith, Bacterial vaginosis and HIV acquisition: a meta-analysis of published studies. *AIDS* **22**, 1493-1501 (2008).
6. C. Gosmann, M. N. Anahtar, S. A. Handley, M. Farcasanu, G. Abu-Ali, B. A. Bowman, N. Padavattan, C. Desai, L. Droit, A. Moodley, M. Dong, Y. Chen, N. Ismail, T. Ndung'u, M. S. Ghebremichael, D. R. Wesemann, C. Mitchell, K. L. Dong, C. Huttenhower, B. D. Walker, H. W. Virgin, D. S. Kwon, Lactobacillus-Deficient Cervicovaginal Bacterial Communities Are Associated with Increased HIV Acquisition in Young South African Women. *Immunity* **46**, 29-37 (2017).
7. N. H. van Teijlingen, L. C. Helgers, R. Sarrami-Forooshani, E. M. Zijlstra-Willems, J. L. van Hamme, C. Segui-Perez, M. Y. van Smoorenburg, H. Borgdorff, J. H. van de Wijgert, E. van Leeuwen, J. A. van der Post, K. Strijbis, C. M. Ribeiro, T. B. Geijtenbeek, Vaginal bacterium Prevotella timonensis turns protective Langerhans cells into HIV-1 reservoirs for virus dissemination. *EMBO J* **41**, e110629 (2022).
8. L. R. Buckner, A. M. Amedee, H. L. Albritton, P. A. Kozlowski, N. Lacour, C. L. McGowin, D. J. Schust, A. J. Quayle, Chlamydia trachomatis Infection of Endocervical Epithelial Cells Enhances Early HIV Transmission Events. *PLoS One* **11**, e0146663 (2016).

9. L. J. P. Liebenberg, L. R. McKinnon, N. Yende-Zuma, N. Garrett, C. Baxter, A. B. M. Kharsany, D. Archary, A. Rositch, N. Samsunder, L. E. Mansoor, J. S. Passmore, S. S. Abdool Karim, Q. Abdool Karim, HPV infection and the genital cytokine milieu in women at high risk of HIV acquisition. *Nat Commun* **10**, 5227 (2019).

10. C. F. Houlihan, N. L. Larke, D. Watson-Jones, K. K. Smith-McCune, S. Shiboski, P. E. Gravitt, J. S. Smith, L. Kuhn, C. Wang, R. Hayes, Human papillomavirus infection and increased risk of HIV acquisition. A systematic review and meta-analysis. *AIDS* **26**, 2211-2222 (2012).

11. R. E. Haaland, P. A. Hawkins, J. Salazar-Gonzalez, A. Johnson, A. Tichacek, E. Karita, O. Manigart, J. Mulenga, B. F. Keele, G. M. Shaw, B. H. Hahn, S. A. Allen, C. A. Derdeyn, E. Hunter, Inflammatory genital infections mitigate a severe genetic bottleneck in heterosexual transmission of subtype A and C HIV-1. *PLoS Pathog* **5**, e1000274 (2009).

12. P. D. Ghys, K. Fransen, M. O. Diallo, V. Ettiegne-Traore, I. M. Coulibaly, K. M. Yeboue, M. L. Kalish, C. Maurice, J. P. Whitaker, A. E. Greenberg, M. Laga, The associations between cervicovaginal HIV shedding, sexually transmitted diseases and immunosuppression in female sex workers in Abidjan, Cote d'Ivoire. *AIDS* **11**, F85-93 (1997).

13. L. F. Johnson, D. A. Lewis, The effect of genital tract infections on HIV-1 shedding in the genital tract: a systematic review and meta-analysis. *Sex Transm Dis* **35**, 946-959 (2008).

14. L. J. Liebenberg, L. Masson, K. B. Arnold, L. R. McKinnon, L. Werner, E. Proctor, D. Archary, L. E. Mansoor, D. A. Lauffenburger, Q. Abdool Karim, S. S. Abdool Karim, J. S. Passmore, Genital-Systemic Chemokine Gradients and the Risk of HIV Acquisition in Women. *J Acquir Immune Defic Syndr* **74**, 318-325 (2017).

15. L. Masson, K. B. Arnold, F. Little, K. Mlisana, D. A. Lewis, N. Mkhize, H. Gamieldien, S. Ngcapu, L. Johnson, D. A. Lauffenburger, Q. Abdool Karim, S. S. Abdool Karim, J. A. Passmore, Inflammatory cytokine biomarkers to identify women with asymptomatic sexually transmitted infections and bacterial vaginosis who are at high risk of HIV infection. *Sex Transm Infect* **92**, 186-193 (2016).

16. L. Masson, J. A. Passmore, L. J. Liebenberg, L. Werner, C. Baxter, K. B. Arnold, C. Williamson, F. Little, L. E. Mansoor, V. Naranbhai, D. A. Lauffenburger, K. Ronacher, G.

Walzl, N. J. Garrett, B. L. Williams, M. Couto-Rodriguez, M. Hornig, W. I. Lipkin, A. Grobler, Q. Abdool Karim, S. S. Abdool Karim, Genital inflammation and the risk of HIV acquisition in women. *Clin Infect Dis* **61**, 260-269 (2015).

17. D. J. Schust, J. A. Ibana, L. R. Buckner, M. Ficarra, J. Sugimoto, A. M. Amedee, A. J. Quayle, Potential mechanisms for increased HIV-1 transmission across the endocervical epithelium during C. trachomatis infection. *Curr HIV Res* **10**, 218-227 (2012).

18. F. Veglia, E. Sanseviero, D. I. Gabrilovich, Myeloid-derived suppressor cells in the era of increasing myeloid cell diversity. *Nat Rev Immunol* **21**, 485-498 (2021).

19. S. J. Park, D. E. Nam, H. C. Seong, Y. S. Hahn, New Discovery of Myeloid-Derived Suppressor Cell's Tale on Viral Infection and COVID-19. *Front Immunol* **13**, 842535 (2022).

20. E. Medina, D. Hartl, Myeloid-Derived Suppressor Cells in Infection: A General Overview. *J Innate Immun* **10**, 407-413 (2018).

21. V. Bronte, S. Brandau, S. H. Chen, M. P. Colombo, A. B. Frey, T. F. Greten, S. Mandruzzato, P. J. Murray, A. Ochoa, S. Ostrand-Rosenberg, P. C. Rodriguez, A. Sica, V. Umansky, R. H. Vonderheide, D. I. Gabrilovich, Recommendations for myeloid-derived suppressor cell nomenclature and characterization standards. *Nat Commun* **7**, 12150 (2016).

22. L. Wang, J. Zhao, J. P. Ren, X. Y. Wu, Z. D. Morrison, M. A. Elgazzar, S. B. Ning, J. P. Moorman, Z. Q. Yao, Expansion of myeloid-derived suppressor cells promotes differentiation of regulatory T cells in HIV-1+ individuals. *AIDS* **30**, 1521-1531 (2016).

23. A. Sacchi, N. Tumino, A. Sabatini, E. Cimini, R. Casetti, V. Bordoni, G. Grassi, C. Agrati, Myeloid-Derived Suppressor Cells Specifically Suppress IFN-gamma Production and Antitumor Cytotoxic Activity of Vdelta2 T Cells. *Front Immunol* **9**, 1271 (2018).

24. N. Tumino, F. Besi, S. Martini, A. L. Di Pace, E. Munari, L. Quatrini, A. Pelosi, P. F. Fiore, G. Fiscon, P. Paci, F. Scordamaglia, M. G. Covesnon, G. Bogina, M. C. Mingari, L. Moretta, P. Vacca, Polymorphonuclear Myeloid-Derived Suppressor Cells Are Abundant in Peripheral Blood of Cancer Patients and Suppress Natural Killer Cell Anti-Tumor Activity. *Front Immunol* **12**, 803014 (2021).

25. M. F. Lampe, C. B. Wilson, M. J. Bevan, M. N. Starnbach, Gamma interferon production by cytotoxic T lymphocytes is required for resolution of Chlamydia trachomatis infection. *Infect Immun* **66**, 5457-5461 (1998).

26. S. C. Fankhauser, M. N. Starnbach, PD-L1 limits the mucosal CD8+ T cell response to Chlamydia trachomatis. *J Immunol* **192**, 1079-1090 (2014).

27. A. N. Russell, X. Zheng, C. M. O'Connell, H. C. Wiesenfeld, S. L. Hillier, B. D. Taylor, M. D. Picard, J. B. Flechtner, W. Zhong, L. C. Frazer, T. Darville, Identification of Chlamydia trachomatis Antigens Recognized by T Cells From Highly Exposed Women Who Limit or Resist Genital Tract Infection. *J Infect Dis* **214**, 1884-1892 (2016).

28. D. C. Gondek, N. R. Roan, M. N. Starnbach, T cell responses in the absence of IFN-gamma exacerbate uterine infection with Chlamydia trachomatis. *J Immunol* **183**, 1313-1319 (2009).

29. S. Falck-Jones, S. Vangeti, M. Yu, R. Falck-Jones, A. Cagigi, I. Badolati, B. Osterberg, M. J. Lautenbach, E. Ahlberg, A. Lin, R. Lepzien, I. Szurgot, K. Lenart, F. Hellgren, H. Maecker, J. Salde, J. Albert, N. Johansson, M. Bell, K. Lore, A. Farnert, A. Smed-Sorensen, Functional monocytic myeloid-derived suppressor cells increase in blood but not airways and predict COVID-19 severity. *J Clin Invest* **131**, (2021).

30. B. V. Kumar, W. Ma, M. Miron, T. Granot, R. S. Guyer, D. J. Carpenter, T. Senda, X. Sun, S. H. Ho, H. Lerner, A. L. Friedman, Y. Shen, D. L. Farber, Human Tissue-Resident Memory T Cells Are Defined by Core Transcriptional and Functional Signatures in Lymphoid and Mucosal Sites. *Cell Rep* **20**, 2921-2934 (2017).

31. J. Cantero-Perez, J. Grau-Exposito, C. Serra-Peinado, D. A. Rosero, L. Luque-Ballesteros, A. Astorga-Gamaza, J. Castellvi, T. Sanhueza, G. Tapia, B. Lloveras, M. A. Fernandez, J. G. Prado, J. M. Sole-Sedeno, A. Tarrats, C. Lecumberri, L. Manalich-Barrachina, C. Centeno-Mediavilla, V. Falco, M. J. Buzon, M. Genesca, Resident memory T cells are a cellular reservoir for HIV in the cervical mucosa. *Nat Commun* **10**, 4739 (2019).

32. D. Chan, P. R. Bennett, Y. S. Lee, S. Kundu, T. G. Teoh, M. Adan, S. Ahmed, R. G. Brown, A. L. David, H. V. Lewis, B. Gimeno-Molina, J. E. Norman, S. J. Stock, V. Terzidou, P. Kropf,

M. Botto, D. A. MacIntyre, L. Sykes, Microbial-driven preterm labour involves crosstalk between the innate and adaptive immune response. *Nat Commun* **13**, 975 (2022).

33. S. Abraham, H. B. Juel, P. Bang, H. M. Cheeseman, R. B. Dohn, T. Cole, M. P. Kristiansen, K. S. Korsholm, D. Lewis, A. W. Olsen, L. R. McFarlane, S. Day, S. Knudsen, K. Moen, M. Ruhwald, I. Kromann, P. Andersen, R. J. Shattock, F. Follmann, Safety and immunogenicity of the chlamydia vaccine candidate CTH522 adjuvanted with CAF01 liposomes or aluminium hydroxide: a first-in-human, randomised, double-blind, placebo-controlled, phase 1 trial. *Lancet Infect Dis* **19**, 1091-1100 (2019).

34. C. Agrati, A. Sacchi, V. Bordoni, E. Cimini, S. Notari, G. Grassi, R. Casetti, E. Tartaglia, E. Lalle, A. D'Abramo, C. Castilletti, L. Marchioni, Y. Shi, A. Mariano, J. W. Song, J. Y. Zhang, F. S. Wang, C. Zhang, G. M. Fimia, M. R. Capobianchi, M. Piacentini, A. Antinori, E. Nicastri, M. Maeurer, A. Zumla, G. Ippolito, Expansion of myeloid-derived suppressor cells in patients with severe coronavirus disease (COVID-19). *Cell Death Differ* **27**, 3196-3207 (2020).

35. T. Vollbrecht, R. Stirner, A. Tufman, J. Roider, R. M. Huber, J. R. Bogner, A. Lechner, C. Bourquin, R. Draenert, Chronic progressive HIV-1 infection is associated with elevated levels of myeloid-derived suppressor cells. *AIDS* **26**, F31-37 (2012).

36. X. Lu, Y. Wang, Y. Ma, D. Huang, Y. Lu, X. Liu, R. Zhou, P. Yu, L. Zhang, J. Chen, R. Lu, F. Wang, YAP1 induces marrow derived suppressor cell recruitment in Chlamydia trachomatis infection. *Immunol Lett* **242**, 8-16 (2022).

37. S. S. Witkin, E. Minis, A. Athanasiou, J. Leizer, I. M. Linhares, Chlamydia trachomatis: the Persistent Pathogen. *Clin Vaccine Immunol* **24**, (2017).

38. M. Elkabets, V. S. Ribeiro, C. A. Dinarello, S. Ostrand-Rosenberg, J. P. Di Santo, R. N. Apte, C. A. Vosshenrich, IL-1beta regulates a novel myeloid-derived suppressor cell subset that impairs NK cell development and function. *Eur J Immunol* **40**, 3347-3357 (2010).

39. Z. G. Fridlender, J. Sun, I. Mishalian, S. Singhal, G. Cheng, V. Kapoor, W. Horng, G. Fridlender, R. Bayuh, G. S. Worthen, S. M. Albelda, Transcriptomic analysis comparing tumor-associated neutrophils with granulocytic myeloid-derived suppressor cells and normal neutrophils. *PLoS One* **7**, e31524 (2012).

40. H. Shi, Y. Qin, Y. Tian, J. Wang, Y. Wang, Z. Wang, J. Lv, Interleukin-1beta triggers the expansion of circulating granulocytic myeloid-derived suppressor cell subset dependent on Erk1/2 activation. *Immunobiology* **227**, 152165 (2022).

41. A. Sacchi, G. Grassi, V. Bordoni, P. Lorenzini, E. Cimini, R. Casetti, E. Tartaglia, L. Marchioni, N. Petrosillo, F. Palmieri, G. D'Offizi, S. Notari, M. Tempestilli, M. R. Capobianchi, E. Nicastri, M. Maeurer, A. Zumla, F. Locatelli, A. Antinori, G. Ippolito, C. Agrati, Early expansion of myeloid-derived suppressor cells inhibits SARS-CoV-2 specific T-cell response and may predict fatal COVID-19 outcome. *Cell Death Dis* **11**, 921 (2020).

42. S. Karakhanova, S. Meisel, S. Ring, K. Mahnke, A. H. Enk, ERK/p38 MAP-kinases and PI3K are involved in the differential regulation of B7-H1 expression in DC subsets. *Eur J Immunol* **40**, 254-266 (2010).

43. S. Su, J. Zhao, Y. Xing, X. Zhang, J. Liu, Q. Ouyang, J. Chen, F. Su, Q. Liu, E. Song, Immune Checkpoint Inhibition Overcomes ADCP-Induced Immunosuppression by Macrophages. *Cell* **175**, 442-457 e423 (2018).

44. S. Kusmartsev, E. Eruslanov, H. Kubler, T. Tseng, Y. Sakai, Z. Su, S. Kaliberov, A. Heiser, C. Rosser, P. Dahm, D. Siemann, J. Vieweg, Oxidative stress regulates expression of VEGFR1 in myeloid cells: link to tumor-induced immune suppression in renal cell carcinoma. *J Immunol* **181**, 346-353 (2008).

45. L. Yang, L. M. DeBusk, K. Fukuda, B. Fingleton, B. Green-Jarvis, Y. Shyr, L. M. Matrisian, D. P. Carbone, P. C. Lin, Expansion of myeloid immune suppressor Gr+CD11b+ cells in tumor-bearing host directly promotes tumor angiogenesis. *Cancer Cell* **6**, 409-421 (2004).

46. M. R. Barros, Jr., C. M. L. de Melo, M. Barros, R. de Cassia Pereira de Lima, A. C. de Freitas, A. Venuti, Activities of stromal and immune cells in HPV-related cancers. *J Exp Clin Cancer Res* **37**, 137 (2018).

47. Y. Liang, W. Wang, X. Zhu, M. Yu, C. Zhou, Inhibition of myeloid-derived suppressive cell function with all-trans retinoic acid enhanced anti-PD-L1 efficacy in cervical cancer. *Sci Rep* **12**, 9619 (2022).

48. M. Z. Noman, G. Desantis, B. Janji, M. Hasmim, S. Karray, P. Dessen, V. Bronte, S. Chouaib, PD-L1 is a novel direct target of HIF-1alpha, and its blockade under hypoxia enhanced MDSC-mediated T cell activation. *J Exp Med* **211**, 781-790 (2014).

49. J. Yu, W. Du, F. Yan, Y. Wang, H. Li, S. Cao, W. Yu, C. Shen, J. Liu, X. Ren, Myeloid-derived suppressor cells suppress antitumor immune responses through IDO expression and correlate with lymph node metastasis in patients with breast cancer. *J Immunol* **190**, 3783-3797 (2013).

50. E. Y. Enioutina, D. Bareyan, R. A. Daynes, A role for immature myeloid cells in immune senescence. *J Immunol* **186**, 697-707 (2011).

51. A. Salminen, K. Kaarniranta, A. Kauppinen, The role of myeloid-derived suppressor cells (MDSC) in the inflammaging process. *Ageing Res Rev* **48**, 1-10 (2018).

52. G. Dong, M. You, H. Fan, J. Ji, L. Ding, P. Li, Y. Hou, 17beta-estradiol contributes to the accumulation of myeloid-derived suppressor cells in blood by promoting TNF-alpha secretion. *Acta Biochim Biophys Sin (Shanghai)* **47**, 620-629 (2015).

53. N. Kostlin, H. Kugel, B. Spring, A. Leiber, A. Marme, M. Henes, N. Rieber, D. Hartl, C. F. Poets, C. Gille, Granulocytic myeloid derived suppressor cells expand in human pregnancy and modulate T-cell responses. *Eur J Immunol* **44**, 2582-2591 (2014).

54. B. G. Reed, B. R. Carr, in *Endotext,* K. R. Feingold *et al.*, Eds. (South Dartmouth (MA), 2000).

55. C. A. Muzny, N. Cerca, J. H. Elnaggar, C. M. Taylor, J. D. Sobel, B. Van Der Pol, State of the Art for Diagnosis of Bacterial Vaginosis. *J Clin Microbiol* **61**, e0083722 (2023).

56. J. Cantero, M. Genesca, Maximizing the immunological output of the cervicovaginal explant model. *J Immunol Methods* **460**, 26-35 (2018).

57. M. A. Scidmore, Cultivation and Laboratory Maintenance of Chlamydia trachomatis. *Curr Protoc Microbiol* **Chapter 11**, Unit 11A 11 (2005).

Acknowledgments: We would like to thank all the patients who participated in the study and Joan Puñet Ortiz and Sara Monreal Peinado for assistance with cell sorting at the Cytomics Platform, UAT, VHIR.

Funding:

This study was funded by:

Fundació La Marató TV3 (FMTV3) grant 201814-10 (MG)

Fundació La Marató TV3 (FMTV3) grant 202112-30 (MG)

Spanish Health Institute Carlos III (ISCIII) co-funded by ERDF/ESF, "A way to make Europe"/"Investing in your future" grant PI20/00160 (MG)

Gilead fellowship grant GLD18/00008 (MG)

Spanish Health Institute Carlos III, Miguel Servet program grant CP17/00179 (MJB)

Vall d'Hebron Institut de Recerca (VHIR) PhD Fellowship (NM)

Author contributions:

Conceptualization: MG

Methodology, DKJP, ABM, NM, JC, YHM, DAS, CR

Patient recruitment and sample collection: VD, MA, PA, JNG, LMB, CCM, NLR, JC, VF

Investigation: DKJP, ABM, NM, JC, MJB

Formal analysis: DKJP, NM, JC, MJB, MG

Supervision: MG

Writing—original draft: DKJP, MG

Writing—review & editing: all authors

Competing interests: The authors declare that they did not receive any third-party payments or services that influenced the submitted work.

Data and materials availability: All data are available in the main text or the supplementary materials.

Figures

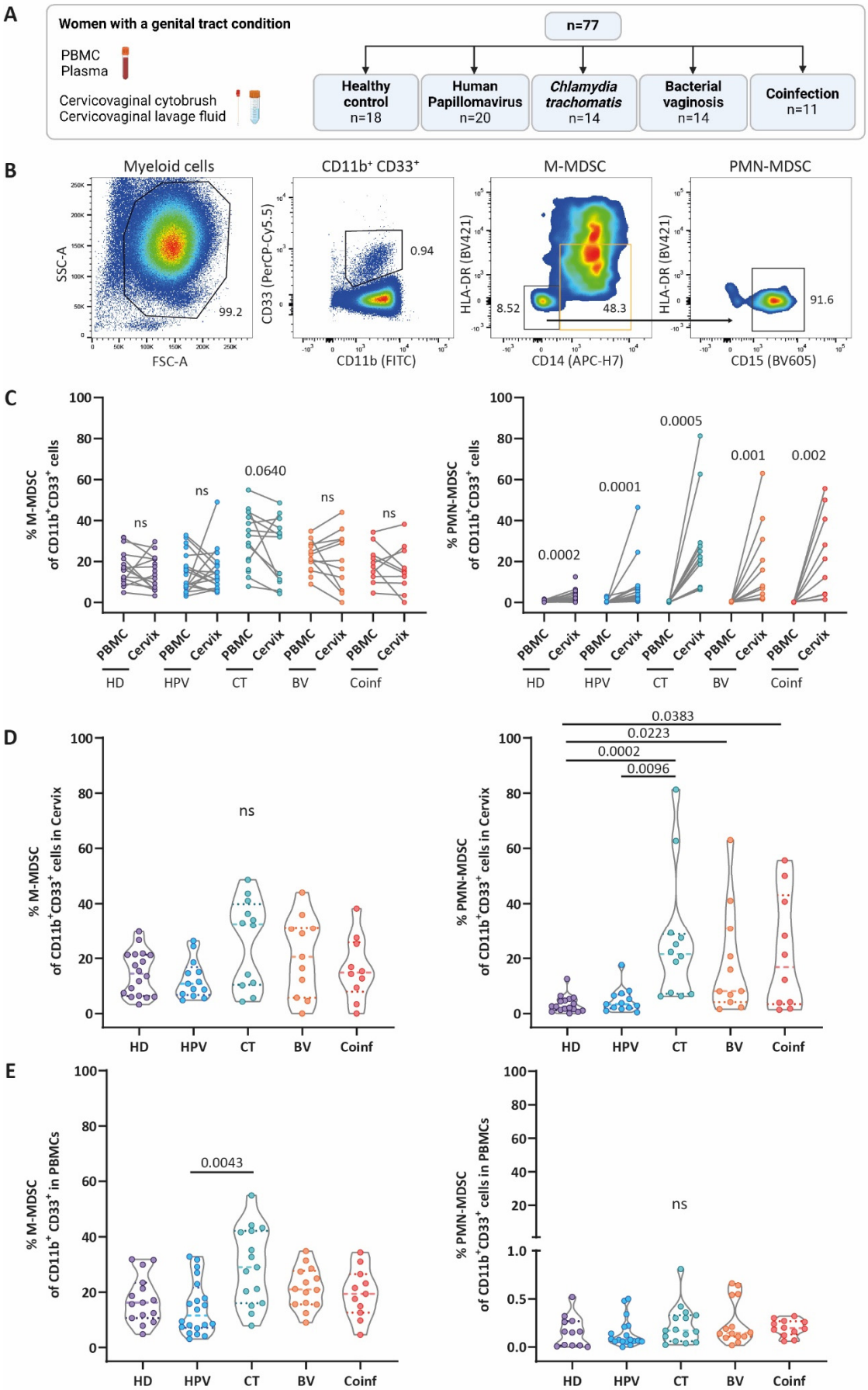
A
Women with a genital tract condition
PBMC
Plasma
Cervicovaginal cytobrush
Cervicovaginal lavage fluid
n=77
Healthy control n=18
Human Papillomavirus n=20
Chlamydia trachomatis n=14
Bacterial vaginosis n=14
Coinfection n=11
B
Myeloid cells
CD11b+ CD33+
M-MDSC
PMN-MDSC
SSC-A
FSC-A
99.2
CD33 (PerCP-Cy5.5)
CD11b (FITC)
0.94
HLA-DR (BV421)
CD14 (APC-H7)
8.52
48.3
CD15 (BV605)
91.6
C
% M-MDSC of CD11b+CD33+ cells
ns
ns
0.0640
ns
ns
% PMN-MDSC of CD11b+CD33+ cells
0.0002
0.0001
0.0005
0.001
0.002
PBMC
Cervix
HD
HPV
CT
BV
Coinf
D
% M-MDSC of CD11b+CD33+ cells in Cervix
ns
% PMN-MDSC of CD11b+CD33+ cells in Cervix
0.0383
0.0223
0.0002
0.0096
HD
HPV
CT
BV
Coinf
E
% M-MDSC of CD11b+ CD33+ in PBMCs
0.0043
% PMN-MDSC of CD11b+CD33+ cells in PBMCs
ns
HD
HPV
CT
BV
Coinf

Fig. 1. ***PMN-MDSC frequencies are increased in the cervical mucosa of Chlamydial, bacterial vaginosis, and coinfected patients.***

(A) Schematic overview of study participants and sample collection. (B) Representative flow-cytometry plots showing the gating strategy of M-MDSCs and PMN-MDSCs in cervical samples. Complete gating strategy is shown in Supplementary Figure 1A. (C-E) Comparison of M-MDSC and PMN-MDSC frequencies amongst $CD11b^{+}CD33^{+}$ myeloid cells found in (C) paired PBMC and cervical samples within each patient by group, (D) in cervical samples of each group, and (E) PBMC samples of each group. Data are shown as paired samples (C) or violin plots with median and quartiles (D, E). Patient characteristics are shown in Supplementary Table 1. Statistical significance was determined by Wilcoxon test (two-sided) (C), and Kruskal-Wallis test with Dunn's post hoc test (two-sided) (D, E). *$p<0.05$; **$p<0.01$; ***$p<0.001$.

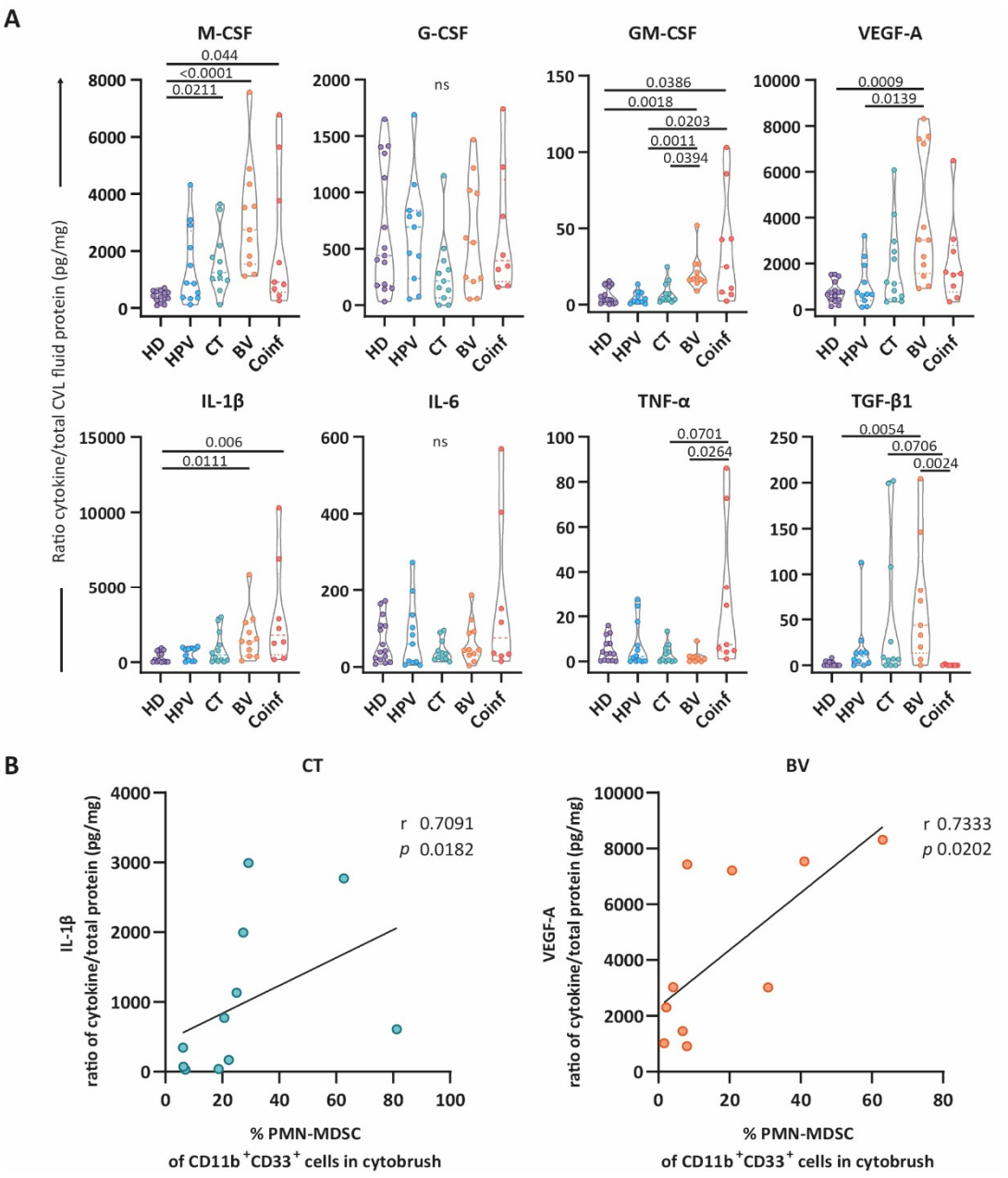

Fig. 2. ***Cytokine and growth factors in cervical lavage fluid.***

(A) Comparison of levels of eight different growth factors and cytokines found in CVL fluid for each group of women included in this study depicted as the ratio of each cytokine per total protein present in the cervical lavage sample. (B) Graphs show the relationship between the level of CVL fluid IL-1β and the frequency of PMN-MDSCs in the cervical samples from CT patients and between the level of CVL fluid VEGF-A and the frequency of PMN-MDSCs in the cervical samples from BV patients. Data are

shown as violin plots with median and quartiles (A) and correlations (*r* and *p* values) assessed by Spearman test (two-sided) (B). Patient characteristics are shown in Supplementary Table 1. Statistical significance was determined by Kruskal-Wallis test with Dunn's post hoc test (two-sided) (A). *p<0.05; **p<0.01; ***p<0.001; ***p<0.0001.

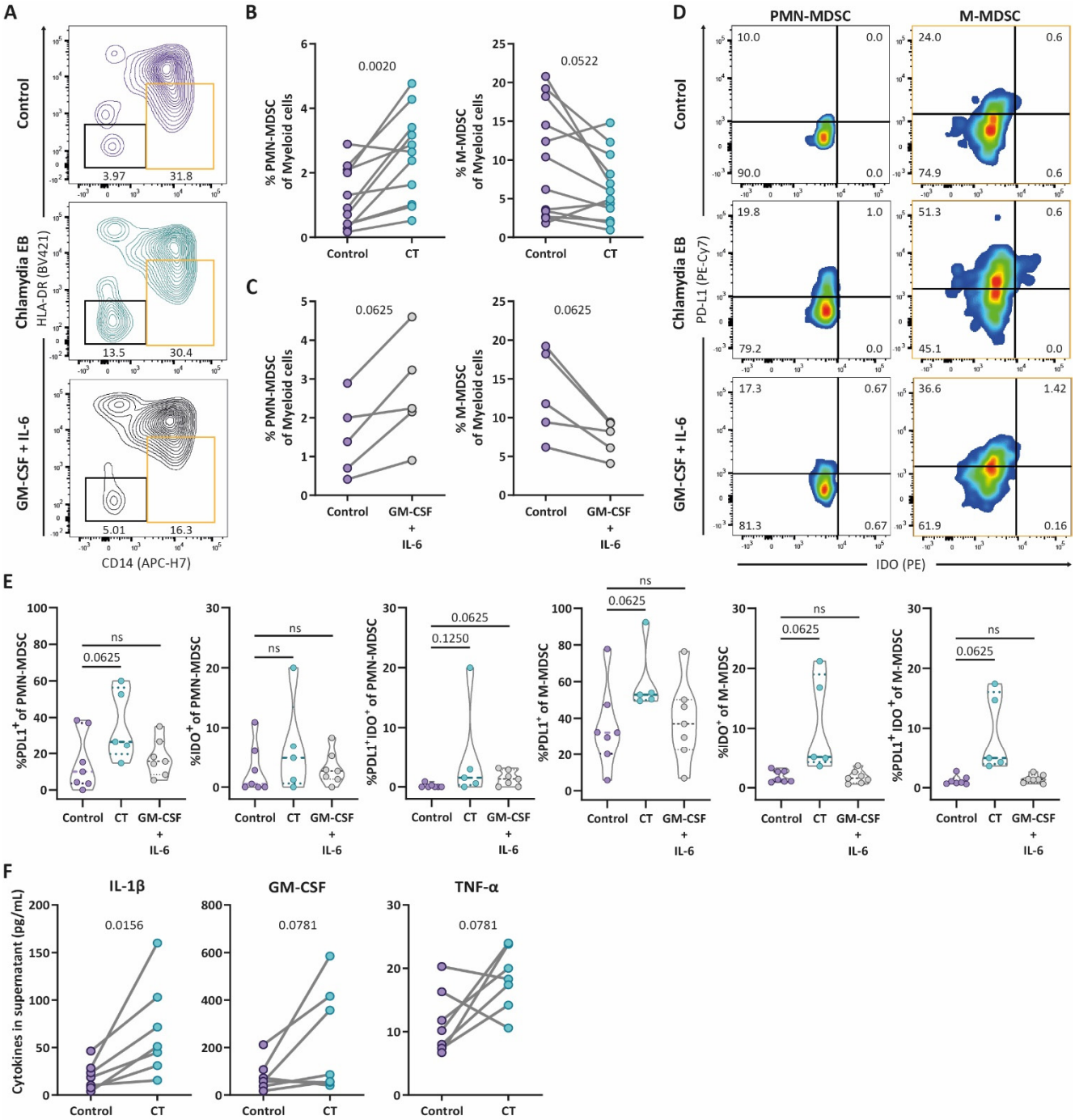

Fig. 3. ***Ex vivo exposure of cervical tissue to C. trachomatis elementary bodies increases PMN-MDSC frequencies and levels of IL-1β.***

(A) Representative flow-cytometry plots showing expression of HLA-DR and CD14 to identify PMN-MDSCs and M-MDSCs after exposure of cervical tissue to *C. trachomatis* elementary bodies (EBs), GM-CSF+IL-6, or control for 48 hours. PMN-MDSCs were confirmed to be $CD15^{+}$ after gating for $HLA\text{-}DR^{-}$ $CD14^{-}$ cells shown in the plot. (B, C) Comparison of the frequency of PMN-MDSCs and M-

MDSCs amongst myeloid cells in cervical tissue exposed to CT EBs (n=11) (B) or GM-CSF+IL-6 (n=5) (C). (D) Representative flow-cytometry plots showing expression of PD-L1 and IDO in PMN-MDSCs and M-MDSCs residing in cervical tissue after exposure to CT EBs for 48 hours compared to the control. (E) Comparison of the frequency of PD-L1^{+}, IDO^{+}, and PD-L1^{+}IDO^{+} PMN-MDSCs and M-MDSCs residing in cervical tissue after exposure to CT EBs or GM-CSF+IL-6 for 48 hours (n=5-7). (F) Comparison of IL-1β, GM-CSF, and TNF-α levels measured in culture supernatant of cervical tissue control *versus* tissue exposed to CT EBs (n=7). Data are shown as paired samples (B, C, F) or violin plots with median and quartiles (E). Statistical significance was determined by Wilcoxon test (two-sided) (B-D and F).

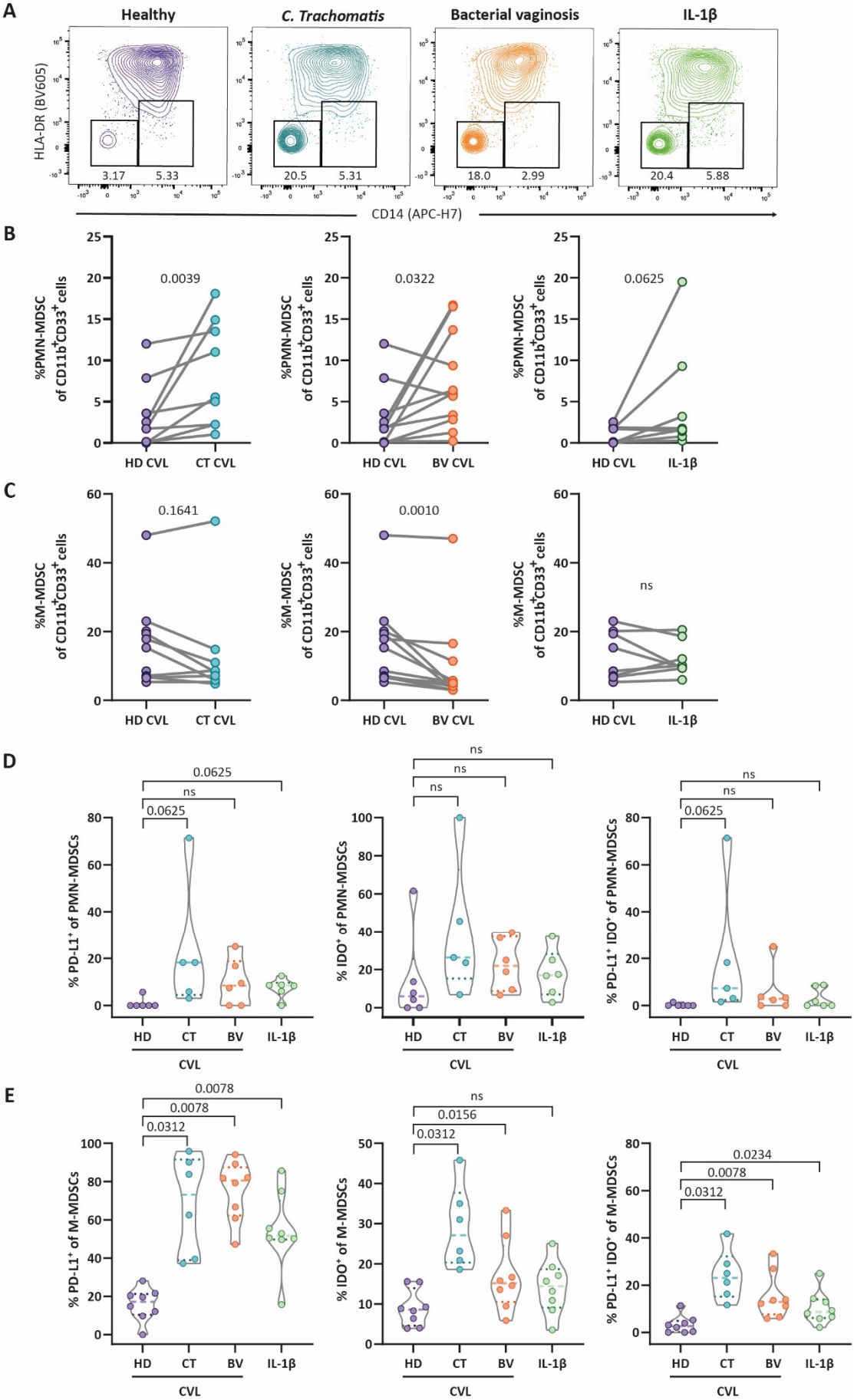
A
Healthy
C. Trachomatis
Bacterial vaginosis
IL-1β
HLA-DR (BV605)
CD14 (APC-H7)
3.17
5.33
20.5
5.31
18.0
2.99
20.4
5.88
B
%PMN-MDSC of CD11b+CD33+ cells
0.0039
0.0322
0.0625
HD CVL
CT CVL
BV CVL
IL-1β
C
%M-MDSC of CD11b+CD33+ cells
0.1641
0.0010
ns
D
% PD-L1+ of PMN-MDSCs
% IDO+ of PMN-MDSCs
% PD-L1+ IDO+ of PMN-MDSCs
0.0625
ns
HD
CT
BV
IL-1β
CVL
E
% PD-L1+ of M-MDSCs
% IDO+ of M-MDSCs
% PD-L1+ IDO+ of M-MDSCs
0.0078
0.0312
0.0156
0.0234

Fig. 4. ***Ex vivo exposure of cervical tissue to genital condition-derived CVL fluid or IL-1β increases PMN-MDSC and PD-L1 frequency.***

(A) Representative flow-cytometry plots showing expression of HLA-DR and CD14 to identify PMN-MDSCs and M-MDSCs after overnight exposure of cervical tissue to CVL fluid derived from HD, CT, or BV patients, or IL-1β. PMN-MDSCs were confirmed to be $CD15^+$ after gating for $HLA\text{-}DR^-$ $CD14^-$ cells shown in the plot. Comparison of the frequency of PMN-MDSCs (B) and M-MDSCs (C) amongst $CD11b^+CD33^+$ myeloid cells in cervical tissue exposed to CVL fluid of HD, CT (n=9), or BV (n=11) patients, or IL-1β (n=8) for 24 hours. Comparison of the frequency of $PD\text{-}L1^+$, IDO^+, and $PD\text{-}L1^+IDO^+$ amongst PMN-MDSCs (D) and M-MDSCs (E) in cervical tissue exposed to CVL fluid of HD (n=6-8), CT (n=5-6), or BV patients (n=6-8), or IL-1β (n=6-8) for 24 hours. Data are shown as paired samples (B, C) or violin plots with median and quartiles (D, E). Statistical significance was determined by Wilcoxon test (two-sided) (B-E).

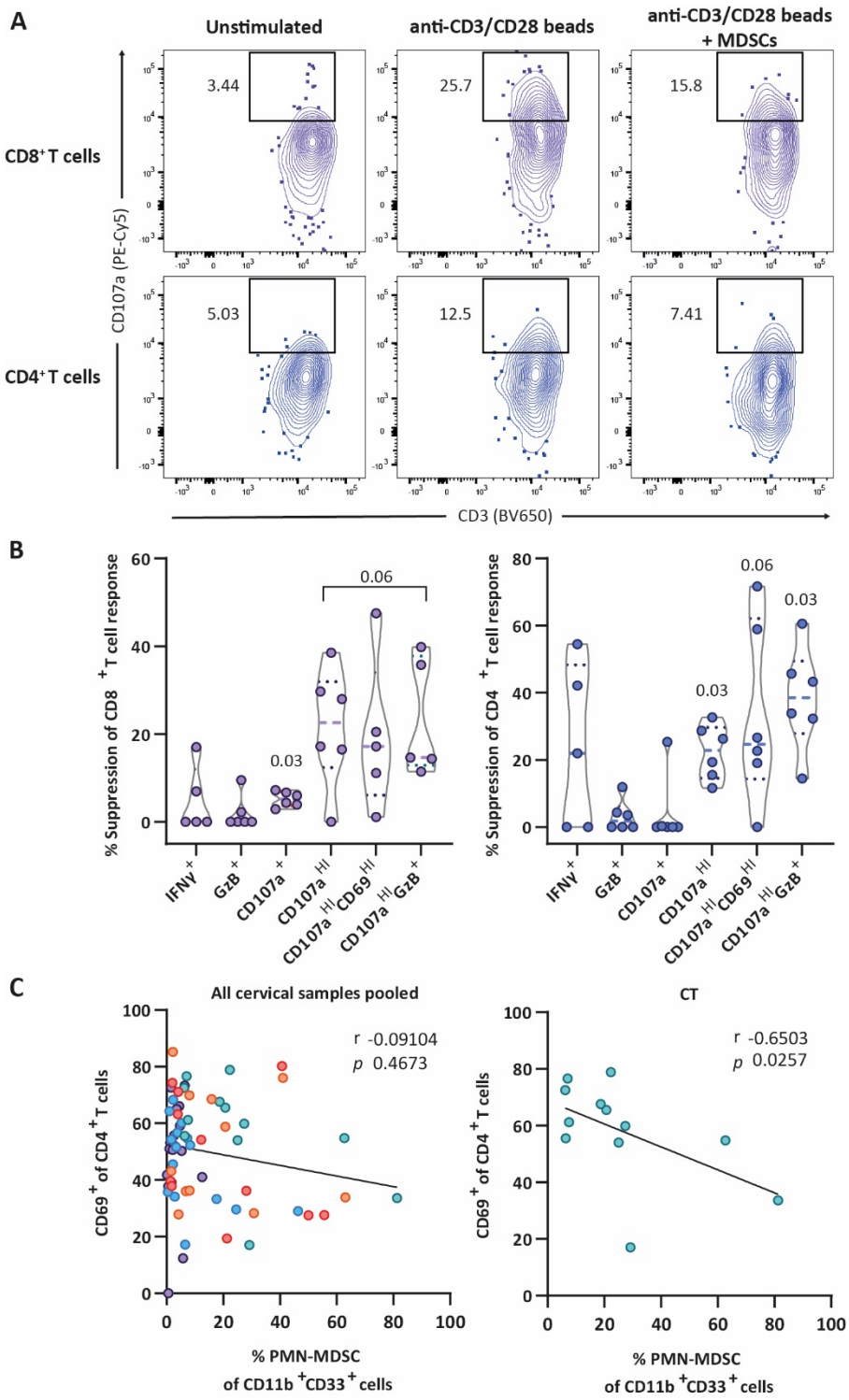

Fig. 5. ***Cervical MDSCs suppress T-cell activation and cytotoxic potential.***

(A) Representative flow-cytometry plots showing CD8$^+$ and CD4$^+$ T cells and their expression of degranulation marker CD107a after exposure to several conditions for 24 hours: unstimulated, anti-CD3/anti-CD28 beads stimulated, and anti-CD3/anti-CD28 beads stimulated in the presence of MDSC

cells (1:5 MDSC to lymphocyte ratio). (B) Calculated percentage of suppression mediated by MDSCs of the indicated markers expressed by $CD8^+$ and $CD4^+$ T cells. (C) Graphs show the relationship between the frequency of $CD69^+$ $CD4^+$ T cells and the frequency of PMN-MDSCs found in the cervix of all included women (left) and of CT patients only (right). Data are shown as violin plots with median and quartiles (B). Statistical significance was determined by Wilcoxon test (two-sided) (B-E). Correlations (*r* and *p* values) were assessed by Spearman test (two-sided) (C).